THE JOURNAL OF BIOLOGICAL CHEMISTRY VOL. 285, NO. 3, pp. 1743–1753, January 15, 2010

Pyk2 Inhibition of p53 as an Adaptive and Intrinsic Mechanism Facilitating Cell Proliferation and Survival*[S]

Received for publication, September 9, 2009, and in revised form, October 26, 2009 Published, JBC Papers in Press, October 30, 2009, DOI 10.1074/jbc.M109.064212

Ssang-Taek Lim[1,2], **Nichol L. G. Miller**[1], **Ju-Ock Nam**[1,3], **Xiao Lei Chen**, **Yangmi Lim**[4], **and David D. Schlaepfer**[5]

From the Department of Reproductive Medicine, Moores Cancer Center, University of California San Diego, La Jolla, California 92093

Pyk2 is a cytoplasmic tyrosine kinase related to focal adhesion kinase (FAK). Compensatory Pyk2 expression occurs upon FAK loss in mice. However, the impact of Pyk2 up-regulation remains unclear. Previous studies showed that nuclear-localized FAK promotes cell proliferation and survival through FAK FERM domain-enhanced p53 tumor suppressor degradation (Lim, S. T., Chen, X. L., Lim, Y., Hanson, D. A., Vo, T. T., Howerton, K., Larocque, N., Fisher, S. J., Schlaepfer, D. D., and Ilic, D. (2008) *Mol. Cell* 29, 9–22). Here, we show that FAK knockdown triggered p53 activation and G_1 cell cycle arrest in human umbilical vein endothelial cells after 4 days. However, by 7 days elevated Pyk2 expression occurred with a reduction in p53 levels and the release of the G_1 block under conditions of continued FAK knockdown. To determine whether Pyk2 regulates p53, experiments were performed in $FAK^{-/-}p21^{-/-}$ mouse embryo fibroblasts expressing endogenous Pyk2 and in ID8 ovarian carcinoma cells expressing both Pyk2 and FAK. In both cell lines, Pyk2 knockdown increased p53 levels and inhibited cell proliferation associated with G_1 cell cycle arrest. Pyk2 FERM domain re-expression was sufficient to reduce p53 levels and promote increased BrdUrd incorporation. Pyk2 FERM promoted Mdm2-dependent p53 ubiquitination. Pyk2 FERM effects on p53 were blocked by proteasomal inhibition or mutational-inactivation of Pyk2 FERM nuclear localization. Staurosporine stress of ID8 cells promoted endogenous Pyk2 nuclear accumulation and enhanced Pyk2 binding to p53. Pyk2 knockdown potentiated ID8 cell death upon staurosporine addition. Moreover, Pyk2 FERM expression in human fibroblasts upon FAK knockdown prevented cisplatin-mediated apoptosis. Our studies demonstrate that nuclear Pyk2 functions to limit p53 levels, thus facilitating cell growth and survival in a kinase-independent manner.

Proline-rich kinase-2 (Pyk2)[6] and focal adhesion kinase (FAK)[6] are related cytoplasmic protein-tyrosine kinases that contain N-terminal 4.1, ezrin, radixin, moesin (FERM), central kinase, proline-rich, and C-terminal focal adhesion targeting domains (1, 2). FAK is abundant and ubiquitously expressed, whereas high level Pyk2 expression is selective and cell type-specific (3). Although Pyk2 and FAK kinase activities can phosphorylate similar targets, they differ in their abilities to promote cell motility (3, 4). In fibroblasts this difference is due to FAK recruitment and activation at integrin-enriched focal adhesion sites, whereas Pyk2 remains primarily perinuclear-distributed (5). Determining the similarities and differences of FAK-Pyk2 action is an area that remains under investigation (6, 7).

FAK knock-out results in an early embryonic lethal phenotype associated with cell proliferation and motility defects (8, 9). During development, loss of FAK results in a p53 tumor suppressor-dependent blockage in mesenchymal cell proliferation (10). Under normal growth conditions, p53 expression is maintained at low levels via polyubiquitination and proteasomal degradation (11). Murine double minute-2 (Mdm2) is a major ubiquitin E3 ligase that regulates p53 levels in cells (12). Nuclear-targeted FAK promotes p53 turnover by facilitating Mdm2-dependent ubiquitination of p53 (10). FAK regulation of p53 levels is dependent upon the FAK FERM domain but independent of FAK kinase activity (13, 14). p53 is a transcription factor that regulates many targets such as the p21Cip/WAF1 (p21) cyclin-dependent kinase inhibitor (15, 16). Importantly, co-inactivation of p21 allows for FAK-null mouse embryo fibroblast (MEF) growth in culture, and these $FAK^{-/-}p21^{-/-}$ MEFs are a unique resource to study mechanisms controlling cell growth and motility in the absence of FAK (13).

In adult mice, endothelial cell (EC)-specific FAK inactivation is associated with increased Pyk2 expression that enables growth factor-stimulated angiogenesis in the absence of FAK (17). Elevated Pyk2 expression also occurs *in vitro* upon FAK inactivation in primary fibroblasts and ECs (17, 18). However, the molecular mechanism(s) of how Pyk2 levels increase and what roles Pyk2 performs upon FAK inactivation remain

* This work was supported, in whole or in part, by National Institutes of Health Grants HL093156 and CA102310 (to D. S.).
[S] The on-line version of this article (available at http://www.jbc.org) contains supplemental Table 1 and Figs. 1 and 2.
[1] These authors contributed equally to this work.
[2] Supported in part by American Heart Association Postdoctoral Fellowship 0725169Y.
[3] Supported in part by Korean Research Foundation Fellowship KRF-2008-357-E00007.
[4] Present address: Mogam Research Institute, 341 Bojeong-dong, Giheung-gu, Yongin 446-799, Korea.
[5] An Established Investigator of the American Heart Association (Grant 0540115N). To whom correspondence should be addressed: University of California San Diego, Moores Cancer Center, Dept. of Reproductive Medicine, 0803, 3855 Health Sciences Dr., La Jolla, CA 92093. Fax: 858-822-7519; E-mail: dschlaepfer@ucsd.edu.

[6] The abbreviations used are: Pyk2, proline-rich kinase 2; Ad, adenovirus; BrdUrd, bromodeoxyuridine; IP, immunoprecipitation; FAK, focal adhesion kinase; FERM, band 4.1, ezrin, radixin, moesin; EC, endothelial cell; ERK, extracellular-regulated kinase; GFP, green fluorescent protein; HA, hemagglutinin; HUVEC, human umbilical vein endothelial cell; Mdm2, murine double minute 2; MEF, mouse embryonic fibroblast; Scr, scrambled; shRNA, short-hairpin RNA; TUNEL, terminal deoxynucleotidyltransferase dUTP nick end-labeling; TT, R184T/R185T; WT, wild type; p5, passage 5.

unclear. We hypothesize that compensatory Pyk2 expression is part of an adaptive or intrinsic cell survival mechanism.

Herein, we establish that Pyk2 in both normal and tumor cells acts to regulate p53 levels controlling both cell proliferation and survival. Pyk2 regulation of p53 occurs in a kinase-independent manner via Pyk2 FERM domain nuclear translocation. Pyk2 FERM forms a complex with p53 and Mdm2 that is weakened by FERM domain F2 lobe mutations. As Pyk2 FERM expression enhances Mdm2-dependent p53 ubiquitination and proteasome inhibitors block Pyk2 effects on p53, our results support a model whereby Pyk2 FERM functions as a scaffold for Mdm2-associated p53 turnover. Moreover, our studies in ovarian carcinoma cells also support the importance of endogenously expressed nuclear-targeted Pyk2 in promoting cell proliferation and survival in cells expressing FAK.

EXPERIMENTAL PROCEDURES

Cells—Early passage $FAK^{-/-}p21^{-/-}$ MEFs and $Mdm2^{-/-}p53^{-/-}$ MEFs were obtained as described via embryo outgrowth (10). Expansion of primary MEFs to two 10-cm plates was achieved after 4- 5 weeks, and this represents passage 5 cells. Human diploid foreskin BJ fibroblasts were from ATCC (CRL-2522), and growth was limited to 50 doublings. Fibroblasts were grown on 0.1% gelatin-coated dishes. 293 and 293T human embryonic kidney cells were used as described (10). Murine ID8 ovarian carcinoma cells were from Katherine Roby (19). All cell lines were maintained in Dulbecco's modified Eagle's medium with 10% fetal bovine serum (Omega Scientific). Human umbilical vein endothelial cells (HUVECs) were from Glycotech and maintained in endothelial growth media (Lonza) with 10% fetal bovine serum and limited to 10 passages.

Antibodies and Reagents—Pyk2 (clone 11) and poly(ADP-ribose) polymerase (clone 42) antibodies were from BD Transduction Laboratories. Mouse p53 (CM5) antibody was from Novocastra. Human p53 (DO-1), p21 (F-5), and extracellular-regulated kinase (ERK) antibodies were from Santa Cruz Biotechnologies. Anti-Ser(P)-15 p53 (16G8) antibody was from Cell Signaling Technologies. Anti-β-actin (AC-17) and anti-FLAG tag (M4) were from Sigma. Anti-Myc (9E10), anti-green fluorescent protein (GFP; B34), and anti-hemagglutinin (HA, 16B12) were from Covance Research. Anti-glyceraldehyde-3-phosphate dehydrogenase (374), anti-FAK (4.47), monoclonal anti-Pyk2 (clone 74), and rabbit polyclonal anti-Pyk2 (06-559) were from Upstate-Millipore. Anti-ubiquitin (FK-2) was from Biomol. Horseradish peroxidase-conjugated anti-mouse and anti-rabbit antibodies were from Pierce/Thermo Scientific. Polyclonal anti-GFP antibodies were generated and used as described (10). Cisplatin and MG132 were from Calbiochem. Propidium iodide was from Sigma. Lipofectamine 2000 (Invitrogen) was used for transfections and staurosporine was from Biovision.

Cloning and Mutagenesis—pEGFP-Pyk2 FERM (residues 39–367) was generated by PCR. pEGFP-Pyk2 FERM R184T/R185T was obtained using QuikChange mutagenesis (Stratagene). The primers used are listed in supplemental Table 1. Both Pyk2 FERM constructs were confirmed by sequencing and cloned into pEGFP-C1 (Clontech).

Lentivirus and Adenovirus Constructs—Human FAK, mouse FAK, mouse Pyk2, and scrambled short-hairpin interference RNA (shRNA) lentiviral vectors (pLentilox 3.7) were created and used as described (10, 20). Full-length adenoviral Myc-tagged human Pyk2 wild-type (WT), autophosphorylation site-mutated (Y402F), and kinase-inactive (R457A) adenovirus were created and used as described (4). Adenoviral Myc-tagged Pyk2 FERM domain wild type and R184T/R185T were generated by PCR and inserted into the pShuttle vector (Stratagene). Constructs were screened by DNA sequencing. Adenovirus was produced using the AdEasy system (Stratagene) and titered and target cells were transduced at a multiplicity of infection between 5 and 25 viral particles per cell to achieve equal expression. shRNA and PCR primers are listed in supplemental Table 1.

Cell Cycle Analysis—Early passage HUVECs were infected with scrambled shRNA or human FAK shRNA lentivirus. After 48 h of lentiviral transduction, cells were trypsinized at day 4 and day 7, fixed with 100% ethanol, and stored at −20 °C until all samples were collected for propidium iodide staining. Cells were collected by centrifugation and washed with phosphate-buffered saline. Cell pellets were resuspended in 300 μl of phosphate-buffered saline containing propidium iodide (10 μg/ml, Sigma) and DNase-free RNase (100 μg/ml, Qiagen) and then incubated at 37 °C with agitation for 1 h. Samples were analyzed by flow cytometry (BD Pharmingen), and cell cycle analyses were performed by ModFit LT3.2 software (Verity Software House).

Cell Proliferation Assay—$FAK^{-/-}p21^{-/-}$ MEFs were infected with scrambled or Pyk2 shRNA lentivirus and incubated for 24 h, then 25,000 cells were plated onto 0.1% gelatin-coated 6-well plates. Cells were harvested every 24 h in triplicate and counted (ViCell, Beckman Coulter). $FAK^{-/-}p21^{-/-}$ cells or ID8 ovarian carcinoma cells were infected with scrambled or FAK shRNA lentivirus and plated onto gelatin-coated glass slides, Ad-Pyk2 FERM expression or transfection of Smartpool mouse p53 small interfering RNA (Dharmacon) was performed at 36 h, and cell proliferation was measured after 72 h by incubation with 10 μM bromodeoxyuridine (BrdUrd) for 16 h. Cells were fixed with 3.7% paraformaldehyde, permeabilized with 0.1% Triton X-100, and incubated with anti-BrdUrd (Roche Applied Science) for 1 h at room temperature followed by Texas Red goat anti-mouse for 30 min. BrdUrd staining was enumerated only for GFP-positive cells. At least 400 GFP-positive cells were counted. Statistical analyses were performed using Prism 5 (GraphPad software).

Ubiquitin Incorporation into p53—Co-transfection experiments were performed in $Mdm2^{+/+}p53^{-/-}$ or $Mdm2^{-/-}p53^{-/-}$ MEFs. First, cells were transduced with Myc-tagged Pyk2 FERM-WT, Pyk2 FERM-TT, or control adenoviral expression vectors, and after 24 h, media were changed, and cells were transfected 1 μg of FLAG-tagged p53 and 0.5 μg of Myc-tagged ubiquitin using FuGENE 6 (Roche Applied Science). At 48 h, MG132 (40 μM) was added 3 h before cell lysis to enhance ubiquitin incorporation. FLAG-p53 was isolated by immunoprecipitation (IP) using FLAG antibody (M4, Sigma) conjugated beads and visualized by anti-ubiquitin (FK-2) blotting.

Cell Apoptosis Assay—Lentivirus-infected human fibroblast apoptosis in the presence or absence of 20 μg/ml cisplatin was measured by terminal deoxynucleotidyltransferase dUTP nick end-labeling (TUNEL) staining using tetramethylrhodamine (Roche Applied Science). Red (TUNEL) and green (GFP-tagged shRNA) fluorescence images were acquired, and the number of cells positive for both GFP and TUNEL were divided by the total number of GFP-positive cells. At least 400 GFP-positive cells were enumerated. ID8 cells were treated with DMSO or staurosporine (1 μM) for the indicated times, collected by trypsinization, stained with allophycocyanin-conjugated annexin V (BD Pharmingen), and analyzed by flow cytometry. Parental ID8 annexin V cell staining was subtracted from all values, and the percentage of annexin V-positive cells was determined from equal numbers of events using the same gate for all time points. Scrambled or anti-FAK shRNA-expressing HUVECs were subjected to annexin V staining and analyzed by flow cytometry at the indicated time points.

Nuclear Localization and Subcellular Fractionation—293T cells were transiently transfected with GFP-Pyk2 FERM wild type or GFP-FERM R184T/R185T, grown on 0.1% gelatin-coated glass coverslips, and fluorescence-visualized (Olympus IX51). Anti-Pyk2 nuclear-associated staining of ID8 cells upon staurosporine addition was visualized using an Olympus IX81 confocal microscope. 293T or ID8 nuclear and cytoplasmic protein fractionation was performed as described (10).

Immunoprecipitation and Immunoblotting—Protein extracts of cells were made using lysis buffer containing 1% Triton X-100, 1% sodium deoxycholate, and 0.1% SDS as described (20). Target proteins were immunoprecipitated with polyclonal GFP or p53 antibodies, collected with immobilized Protein A (RepliGen), and washed in 20 mM Hepes, pH 7.4, 150 mM NaCl, 0.1% Triton, and 10% glycerol at 4 °C. Immunoprecipitated proteins or cell lysate proteins were separated by SDS-PAGE, and sequential immunoblotting was performed as described (10). Relative protein expression levels were measured by analyzing densitometry of blots using ImageJ (Version 1.34s).

RESULTS

Elevated Pyk2 Expression in HUVECs upon FAK Knockdown Coincides with Reduced p53 Levels and Cell Cycle Regulation—Pyk2 levels were found elevated in heart tissue from inducible EC-specific FAK knock-out mice (17), and we found that Pyk2 levels are also elevated in i-EC-FAK-KO lung tissue lysates compared with WT mice (Fig. 1*A*). As FAK has been linked to the regulation of cell cycle progression (21–23), we hypothesize that elevated Pyk2 levels upon FAK inactivation may similarly function to regulate cell proliferation. To test this connection in ECs, HUVECs were transduced with lentiviral scrambled (Scr) or anti-FAK shRNA and evaluated for changes in protein expression (Fig. 1, *B* and *C*) or cell cycle progression (Fig. 1*D*) after 4 or 7 days.

By day 4, immunoblotting revealed that FAK knockdown was ~70% with no change in Pyk2 levels. p53 expression and activation were elevated as determined by total and phospho-Ser15 anti-p53 blotting in FAK shRNA compared with Scr shRNA-expressing cells (Fig. 1*B*). FAK knockdown cells exhibited increased G_0/G_1 with decreased S and G_2/M DNA content (Fig. 1*D*). FAK knockdown did not trigger HUVEC apoptosis, and similar results were obtained with a second FAK shRNA (supplemental Table 1 and Fig. 1). These results are consistent with FAK knockdown resulting in a G_1 cell cycle block with p53 activation potentially acting as a checkpoint preventing efficient cell cycle progression.

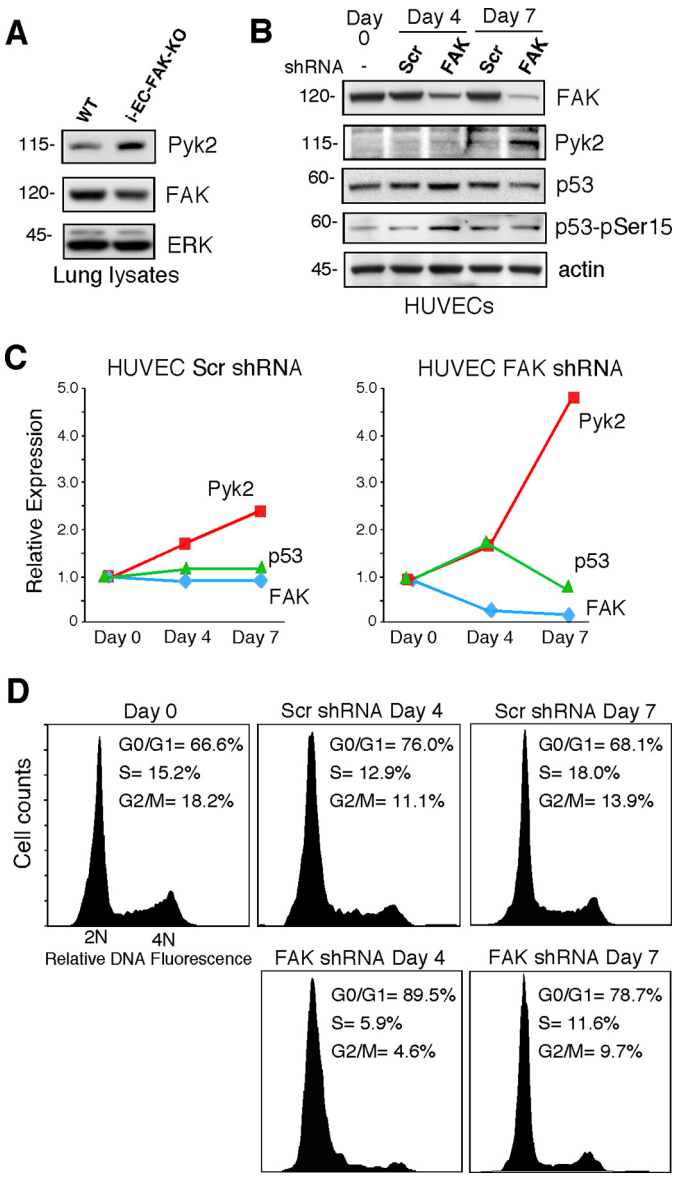

FIGURE 1. **Elevated Pyk2 levels in mouse lung tissue and HUVECs upon FAK inactivation; association with p53 and cell cycle regulation.** *A*, lung tissue lysates from WT and inducible EC-specific FAK knock-out mice were analyzed by anti-Pyk2 and -FAK blotting. Levels of ERK were used as a loading control. *B*, FAK, Pyk2, p53-phosphoserine-15 (*pSer15*), and p53 levels after lentiviral-mediated anti-FAK or control Scr shRNA expression in HUVECs are shown. Actin was used as a loading control. Day 0 represents growing cells just before infection, and days 4 or 7 are times after infection. *C*, densitometric analyses are shown of Pyk2 (*red squares*), p53 (*green triangles*), and FAK (*blue diamonds*) expression in Scr- or FAK shRNA HUVEC lysates (from *panel B*) with values normalized to actin and day 0 levels set to 1. *D*, shown is cell cycle analysis as determined by propidium iodide staining and flow cytometry. Day 0 represents growing cells before lentiviral shRNA expression. FAK but not Scr shRNA-expressing HUVECs exhibit cell cycle arrest (increased G_1 to S ratio) at day 4. Increased percentages of FAK shRNA-expressing cells are in S and G_2/M phases of the cell cycle at day 7 compared with day 4. Cell cycle analyses are representative of two independent experiments. Immunoblots are from one of three independent experiments.

By day 7 FAK knockdown was maximal at ~90%. However, Pyk2 levels were elevated compared with Scr shRNA controls at day 7 (Fig. 1, *B* and *C*). Notably, p53 expression and activation did not differ between FAK- and Scr shRNA-expressing HUVECs at day 7. Moreover, an increased percentage of FAK shRNA cells possessed S and G_2/M DNA content compared with day 4 FAK shRNA HUVECs, which exhibited a G_1 cell cycle block (Fig. 1*D*). These results support the notion that compensatory changes in Pyk2 levels may inhibit p53 and, thus, promote cell cycle progression in HUVECs under conditions of reduced FAK expression.

Pyk2 Regulation of FAK$^{-/-}$p21$^{-/-}$ MEF Proliferation—To test whether Pyk2 can regulate p53 as well as cell growth, experiments need to be performed in cells that lack FAK. However, FAK$^{-/-}$ MEFs do not readily proliferate (8, 10). We found that inactivation of the cell cycle inhibitory p21 protein allows for primary FAK$^{-/-}$p53$^{+/+}$ MEF growth (10). These MEFs are isolated from E8.0 embryos, and passage 5 (p5) cells represent the expansion of MEFs to a 10-cm dish. Analysis of p5 FAK$^{-/-}$p21$^{-/-}$ MEFs revealed low levels of Pyk2 and moderate levels of p53 (Fig. 2*A*). Between p5 and p10, FAK$^{-/-}$p21$^{-/-}$ MEFs exhibited accelerated growth (data not shown). Consistent with the above HUVEC results, analysis of p10 FAK$^{-/-}$p21$^{-/-}$ MEFs lysates revealed elevated Pyk2 and decreased p53 levels compared with earlier passage (Fig. 2*A*).

To determine whether Pyk2 expression changes affect p53 levels and cell proliferation, lentiviral Scr or Pyk2 shRNA were expressed in p10 FAK$^{-/-}$p21$^{-/-}$ MEFs. Pyk2 knockdown resulted in elevated p53 levels (Fig. 2*A*) and the inhibition of cell proliferation (Fig. 2*B*). Cell cycle analyses revealed increased G_0/G_1 with decreased S and G_2/M DNA content compared with Scr controls (Fig. 2*C*). Pyk2 knockdown did not lead to increased cell apoptosis, and similar results were obtained with a second Pyk2 shRNA (supplemental Fig. 2). These results implicate Pyk2 in the regulation of both p53 and cell proliferation in the absence of FAK.

p53 Controls FAK$^{-/-}$p21$^{-/-}$ MEF Cell Cycle Progression—To determine the role of elevated p53 levels upon Pyk2 knockdown, FAK$^{-/-}$p21$^{-/-}$ MEFs were transduced with Scr or Pyk2 shRNA and then transfected with anti-p53 small interfering RNA (*siRNA*; Fig. 3*A*). As the shRNA-containing lentivirus expresses GFP as a cell marker, lentiviral-expressing cells can be directly analyzed for effects on cell cycle progression via enumerating GFP and BrdUrd incorporation into cells (Fig. 3, *B* and *C*). As expected, knockdown of Pyk2 was accompanied by elevated p53 levels (Fig. 3*A*). This corresponded to a 4-fold reduction in FAK$^{-/-}$p21$^{-/-}$ MEF BrdUrd incorporation (Fig. 3, *B* and *C*). Co-inactivation of p53 upon Pyk2 knockdown enhanced BrdUrd incorporation 3-fold compared Pyk2 knockdown cells. As Pyk2 knockdown promotes a G_0/G_1 cell cycle block of FAK$^{-/-}$p21$^{-/-}$ MEFs (Fig. 2*C*), increased BrdUrd incorporation upon p53 inactivation is consistent with a release of the G_0/G_1 block and initiation of cell cycle progression.

Pyk2 FERM Regulation of p53 Levels and FAK$^{-/-}$p21$^{-/-}$ MEF BrdUrd Incorporation—Previous studies demonstrated that the FAK N-terminal FERM domain acts as a nuclear-localized scaffold to promote Mdm2-dependent p53 ubiquitination leading to enhanced p53 proteasomal degradation

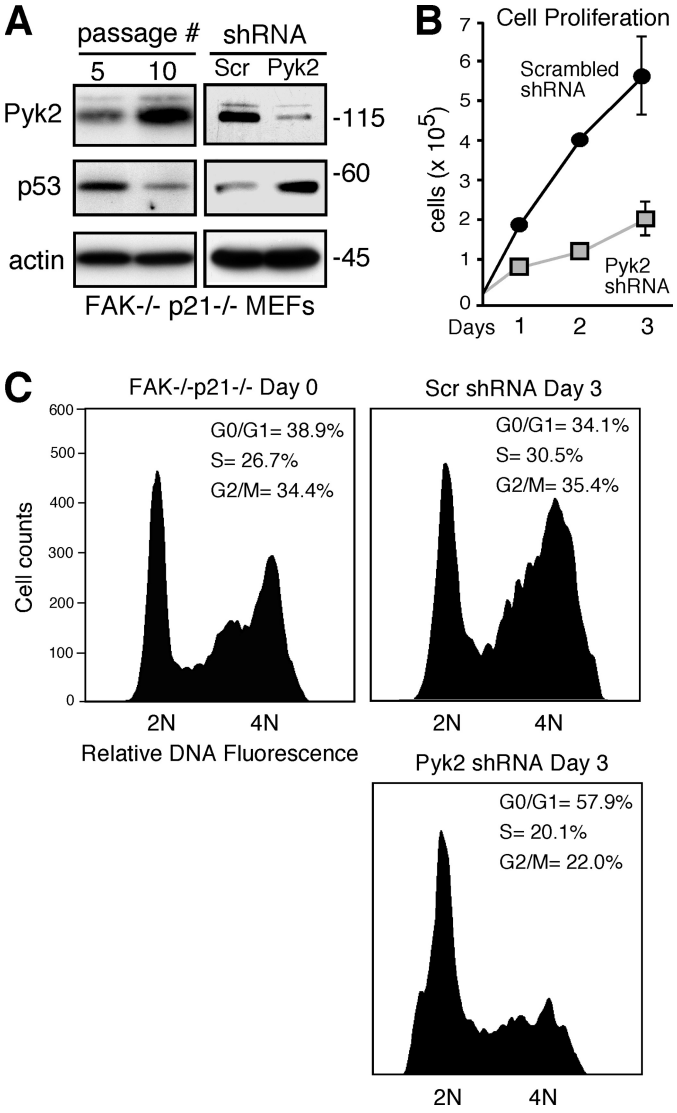

FIGURE 2. **Pyk2 regulation of p53 and growth of FAK$^{-/-}$p21$^{-/-}$ MEFs.** *A*, *left panel*, increased Pyk2 and decreased p53 levels as a function of FAK$^{-/-}$p21$^{-/-}$ MEF passage are shown. *Passage 5* represents expansion of primary FAK$^{-/-}$p21$^{-/-}$ MEFs to a 10-cm dish. *Right panel*, shRNA-mediated Pyk2 knockdown is associated with elevated p53 levels in p10 FAK$^{-/-}$p21$^{-/-}$ MEFs compared with Scr shRNA as determined by anti-Pyk2, p53 and actin blotting. *B*, Pyk2 shRNA-expressing FAK$^{-/-}$p21$^{-/-}$ MEFs grow slower than scrambled shRNA control. Results are the mean cell number ± S.D., $n = 3$ experiments. *C*, cell cycle analysis by propidium iodide staining and flow cytometry is shown. Day 0 represents growing cells before lentiviral shRNA expression. Pyk2 but not Scr shRNA-expressing FAK$^{-/-}$p21$^{-/-}$ MEFs exhibit G_1 cell cycle arrest after 72 h. shRNA-associated experiments were repeated at least two times.

(10). To determine whether Pyk2 FERM can regulate p53, FAK$^{-/-}$p21$^{-/-}$ MEFs were transduced with Scr or Pyk2 shRNA followed by transduction with an adenovirus (Ad) re-expressing human Myc-tagged Pyk2 FERM (residues 39–367). Pyk2 knockdown resulted in elevated p53 levels and significantly reduced FAK$^{-/-}$p21$^{-/-}$ MEF BrdUrd incorporation (Fig. 3, *D* and *E*). Pyk2 FERM re-expression in Pyk2 shRNA-expressing MEFs resulted in decreased steady-state p53 levels and increased BrdUrd incorporation. This is consistent with Pyk2 FERM promoting increased G_1 to S cell cycle progression compared with Pyk2 shRNA-expressing FAK$^{-/-}$p21$^{-/-}$ MEFs. These results support the notion that

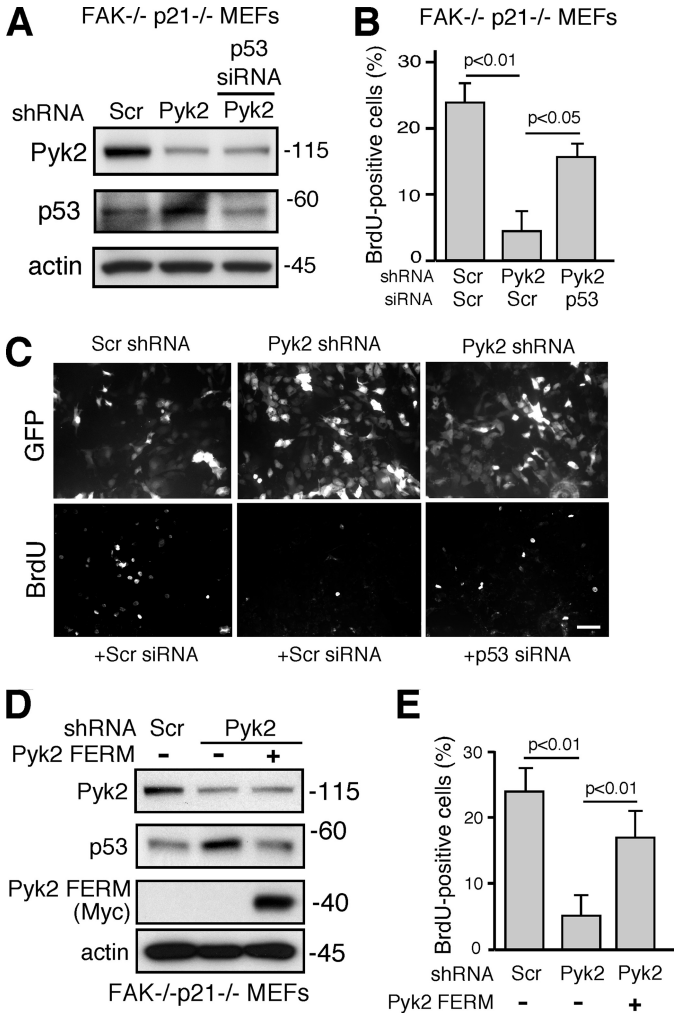

FIGURE 3. **FAK$^{-/-}$p21$^{-/-}$ MEF cell cycle progression is regulated by Pyk2 FERM and p53.** *A*, shown is combined p53 and Pyk2 knockdown. FAK$^{-/-}$p21$^{-/-}$ MEFs were infected with Scr or Pyk2 lentiviral-associated shRNA and, after 24 h, transfected with p53 small interfering RNA (*siRNA*) as indicated. At 96 h, lysates were analyzed by anti-Pyk2, p53, and actin immunoblotting. *B* and *C*, p53 knockdown bypasses proliferation block after Pyk2 knockdown. Cells were transduced with lentiviral shRNA and transfected with p53 small interfering RNA as in *panel A*. After 72 h BrdUrd was added for 16 h, and cells were processed for BrdUrd antibody staining. Results are the mean values ± S.D.; $n = 2$ experiments are the percent of total GFP (from lentiviral shRNA) positive cells. *Panel C* shows representative BrdUrd-stained images. The *scale bar* is 200 μm. *D*, Pyk2 FERM domain expression reduces p53 levels. FAK$^{-/-}$p21$^{-/-}$ MEFs were infected with lentiviral-associated Scr or Pyk2 shRNA and, after 48 h, exposed to either mock or adenoviral Myc-Pyk2 FERM (39–367). At 96 h, lysates were analyzed by anti-Pyk2, p53, Myc (for FERM detection), and actin immunoblotting. *E*, exogenous Pyk2 FERM expression bypasses proliferation block after Pyk2 knockdown. Cells were processed as in *panel D*, and after 72 h BrdUrd was added for 16 h, and then cells were stained with BrdUrd antibody. Mean values ± S.D., $n = 2$ independent experiments are the percent of total GFP (from lentiviral shRNA)-positive cells. *B* and *E*, significance was determined using analysis of variance and Tukey-Kramer HSD tests. shRNA-associated experiments were repeated at least two times.

Pyk2 controls FAK$^{-/-}$p21$^{-/-}$ MEF proliferation in part through Pyk2 FERM effects on p53.

Pyk2 FERM Regulates p53 Independent of Pyk2 Kinase Activity—Structural analyses of the FAK FERM domain reveal that it makes inhibitory contacts with the FAK kinase domain (24). As the Pyk2 FERM domain can also function to inhibit Pyk2 activity (25), and because low levels of Pyk2 remain after Pyk2 shRNA expression in cells, it is possible that FERM-mediated inhibition of Pyk2 kinase activity may affect p53 levels. To test this possibility, Myc-tagged full-length Pyk2 WT, kinase-dead Pyk2 (A457), and a Pyk2 auto-phosphorylation mutant (F402) (Fig. 4*A*) were expressed in human fibroblasts by Ad-mediated transduction, and effects on steady-state p53 levels were determined by immunoblotting (Fig. 4*B*). WT Pyk2 moderately reduced p53 levels, whereas kinase-dead or F402 Pyk2 overexpression resulted in a dramatic reduction of p53 levels. These results show that Pyk2 regulation of p53 is independent of Pyk2 kinase activity.

To determine which residues within the Pyk2 FERM domain are needed for p53 regulation, sequence comparisons were made to the FAK FERM (Fig. 4*A*). FERM domains are composed of three lobes (F1, F2, and F3), and the highest degree of conservation between Pyk2 and FAK (50.4% identity) is within the F2 lobe. Importantly, mutation of FAK FERM at Arg-177 and -R178 to alanine (R177A/R178A) disrupts FAK FERM nuclear localization and p53 regulation (10). These residues are conserved within the Pyk2 F2 lobe at Arg-184 and -185. To test the importance of these sites, they were mutated to threonine (R184T/R185T, designated TT) (Fig. 4*A*). Ad-mediated Pyk2 FERM-TT did not reduce p53 levels as did FERM-WT (Fig. 4*C*). These results support the importance of Pyk2 Arg-184/185 within the FERM F2 lobe in mediating p53 regulation.

Pyk2 FERM-mediated Nuclear Localization—Both FAK and Pyk2 localize to the nucleus in the presence of the nuclear export inhibitor leptomycin B and in response to specific cellular stimuli (13, 26, 27). The bipartite nuclear localization sequence within the F2 lobe of the FAK FERM domain is also conserved within Pyk2 (10), but the functional relevance of this has not been tested. To determine whether the TT mutation within the Pyk2 FERM F2 lobe disrupts nuclear localization, GFP fusions of Pyk2 FERM-WT and Pyk2 FERM-TT were evaluated by fluorescent localization (Fig. 4*D*) and cellular fractionation (Fig. 4*E*). Pyk2 FERM-WT was nuclear-localized in both assays, whereas the majority of Pyk2 FERM-TT was cytoplasmically distributed. As identified nuclear export sequences are conserved between FAK and Pyk2 (28), these results indicate that similar mechanisms may govern FAK and Pyk2 nuclear-cytoplasmic distributions.

Pyk2 FERM Interaction with p53 and Mdm2—As Pyk2 FERM reduces p53 levels, co-IP experiments were performed to determine whether Pyk2 FERM associates with p53 or Mdm2 (Fig. 4, *F–H*). After transient transfection of GFP, GFP-Pyk2 FERM WT, or GFP-Pyk2 FERM-TT into 293 cells, endogenous p53 strongly associated with WT Pyk2 FERM but only weakly with Pyk2 FERM-TT (Fig. 4*F*). A similar result was obtained upon co-transfection of GFP-Pyk2 FERM constructs with HA-tagged Mdm2 (Fig. 4*G*). No specific binding was observed with GFP control-transfected cells, and no binding of p53 was detected in co-IP assays with the GFP-tagged FERM domain from talin (Fig. 4*H*). Thus, FERM-mediated association with p53 and Mdm2 is conserved between Pyk2 and FAK but not with talin.

Pyk2 FERM Promotes Mdm2-dependent p53 Ubiquitination—p53 levels in cells are regulated by a balance between protein expression and degradation (11). The addition of the MG132 proteasome inhibitor for 3 h before cell lysis blocked

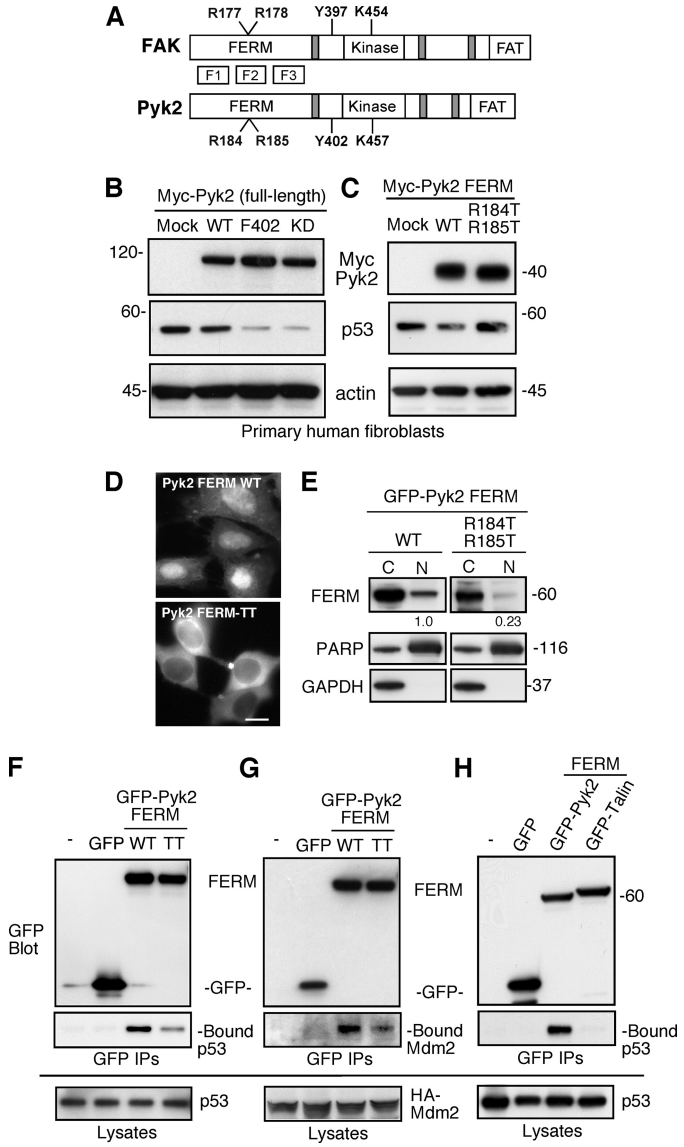

FIGURE 4. **Pyk2 FERM localizes to the nucleus, forms a complex with p53 and Mdm2, and acts to regulate p53 levels in a kinase-independent manner.** *A*, shown is a model depicting FAK and Pyk2 similarities. Both proteins contain an N-terminal FERM domain composed of three subdomains (F1, F2, and F3 lobes), central kinase domains, proline-rich motifs (*shaded boxes*), and C-terminal focal adhesion targeting (*FAT*) domains. FAK Tyr-397 (*Y397*) and Pyk2 Tyr-402 (*Y402*) are conserved autophosphorylation sites, and FAK Lys-454 (*K454*) and Pyk2 Lys-457 (*K457*) within the kinase domain are necessary for ATP binding. Mutation of Arg-177 (*R177*) and Arg-178 (*R178*) within the FAK F2 lobe FERM domain disrupts FAK FERM-mediated regulation of p53 (10) and analogous residues Arg-184 (*R184*) and Arg-185 (*R185*) are present within the F2 lobe of the Pyk2 FERM domain. *B*, Pyk2 reduces p53 levels in a kinase-independent manner. Ad-mediated full-length Pyk2 WT, autophosphorylation site-mutated Pyk2 (*F402*), and kinase-inactive Pyk2 (*R457*) effects on endogenous p53 were detected by anti-Myc, p53, and actin blotting of human fibroblast lysates. *KD*, kinase-dead. *C*, Ad-mediated Pyk2 FERM WT (residues 39–367) but not F2-lobe mutant (R184T and R185T) Pyk2 FERM overexpression decreases endogenous p53 levels in human fibroblasts as determined by immunoblotting. Ad-pShuttle was used as a Mock control. *D*, transiently transfected human 293T cells show that GFP-Pyk2 FERM (39–367) exhibits nuclear accumulation, whereas GFP-Pyk2 FERM (R184T and R185T, TT) containing F2 lobe point mutations remains cytoplasmically distributed. The *scale bar* is 20 μm. *E*, cell fractionation of transiently transfected 293T cells into cytoplasmic (*C*) and nuclear (*N*) fractions reveals nuclear partitioning of GFP-Pyk2 FERM WT but not of GFP-Pyk2 FERM TT. Anti-GFP blotting was used to detect GFP-Pyk2 FERM. Poly(ADP-ribose) polymerase (*PARP*) and glyceraldehyde-3-phosphate dehydrogenase (*GAPDH*) blotting was used to verify nuclear and cytoplasmic fractionation, respectively. *Numbers below the immunoblot panels* represent densitometric analyses of nuclear Pyk2 FERM normalized to poly-(ADP-ribose) polymerase with WT Pyk2 FERM levels set to 1.0. *F*, F2 lobe mutation in Pyk2 weakens the association with endogenous p53. Shown is 293 cell transfection with GFP, GFP-Pyk2 FERM WT, or GFP-Pyk2 FERM (R184T and R185T, TT). p53 association with Pyk2 FERM was detected by co-IP using anti-GFP antibodies and immunoblotting for GFP (*top*) and p53 (*middle*). Total endogenous p53 levels in lysates is shown (*bottom*). *G*, F2 lobe mutation in Pyk2 weakens the interaction with Mdm2. 293 cells were co-transfected with HA-tagged Mdm2 and GFP or GFP-Pyk2 FERM constructs as above. Mdm2 association with Pyk2 FERM was detected by co-IP using anti-GFP antibodies (*top*) and anti-HA tag immunoblotting for Mdm2 (*middle*). Total HA-Mdm2 levels in lysates is shown (*bottom*). *H*, talin FERM does not bind p53. 293 cells were transfected with GFP, GFP-Pyk2 FERM, or GFP-talin FERM, and p53 association was detected by co-IP using anti-GFP antibodies and immunoblotting for GFP (*top*) and p53 (*middle*). Endogenous p53 levels in lysates are shown (*bottom*). Overexpression, fractionation, and co-IP studies were repeated at least two times.

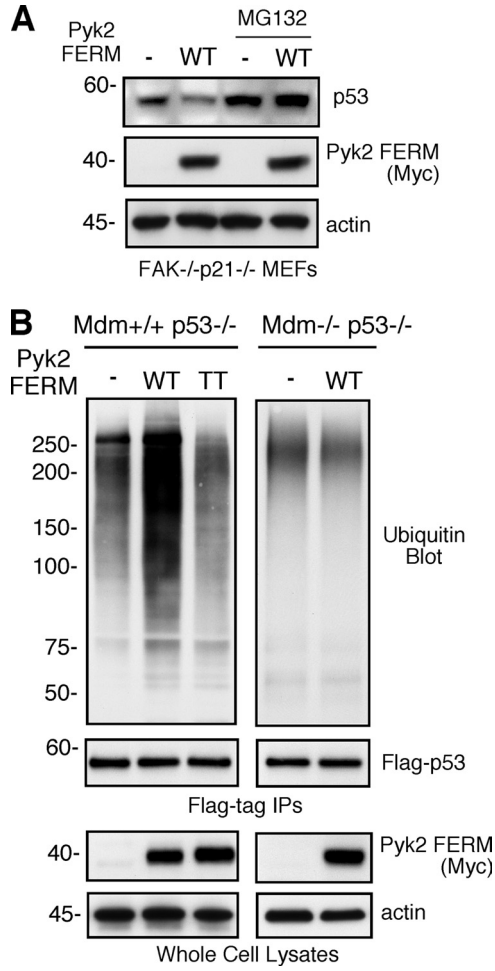

FIGURE 5. **Pyk2 FERM enhances Mdm2-dependent p53 ubiquitination.** *A*, MG132 proteasomal inhibition blocks Pyk2 FERM effects on p53. FAK$^{-/-}$p21$^{-/-}$ MEFs were transduced with Ad-vector (−) or Ad-Myc Pyk2 FERM WT for 48 h. MG132 (40 μM) was added (3 h) before cell lysis, and immunoblotting was performed with p53, Myc (Pyk2 FERM), and actin antibodies. *B*, Mdm2 is required for FERM-enhanced p53 ubiquitination. Mdm2$^{+/+}$p53$^{-/-}$ or Mdm2$^{-/-}$p53$^{-/-}$ MEFs were transduced with Ad-vector (−), Pyk2 FERM-WT, or Pyk2 FERM-TT adenoviral expression vectors followed by transfection with FLAG-tagged p53 and Myc-ubiquitin. MG132 was added 3 h before lysis, and p53 IPs were analyzed by anti-ubiquitin and FLAG-tagged blotting. In cell lysates Myc immunoblotting detected Pyk2 FERM levels, and anti-actin was used for loading controls. Experiments were repeated two times.

Pyk2 FERM effects on p53 (Fig. 5*A*), supporting the conclusion that Pyk2 FERM facilitates p53 turnover. To evaluate Pyk2 FERM effects on p53 ubiquitination, FLAG-p53 was transfected in Mdm2$^{+/+}$p53$^{-/-}$ and Mdm2$^{-/-}$p53$^{-/-}$ MEFs and transduced with Ad-Pyk2 FERM-WT and Ad-Pyk2 FERM-TT (Fig. 5*B*).

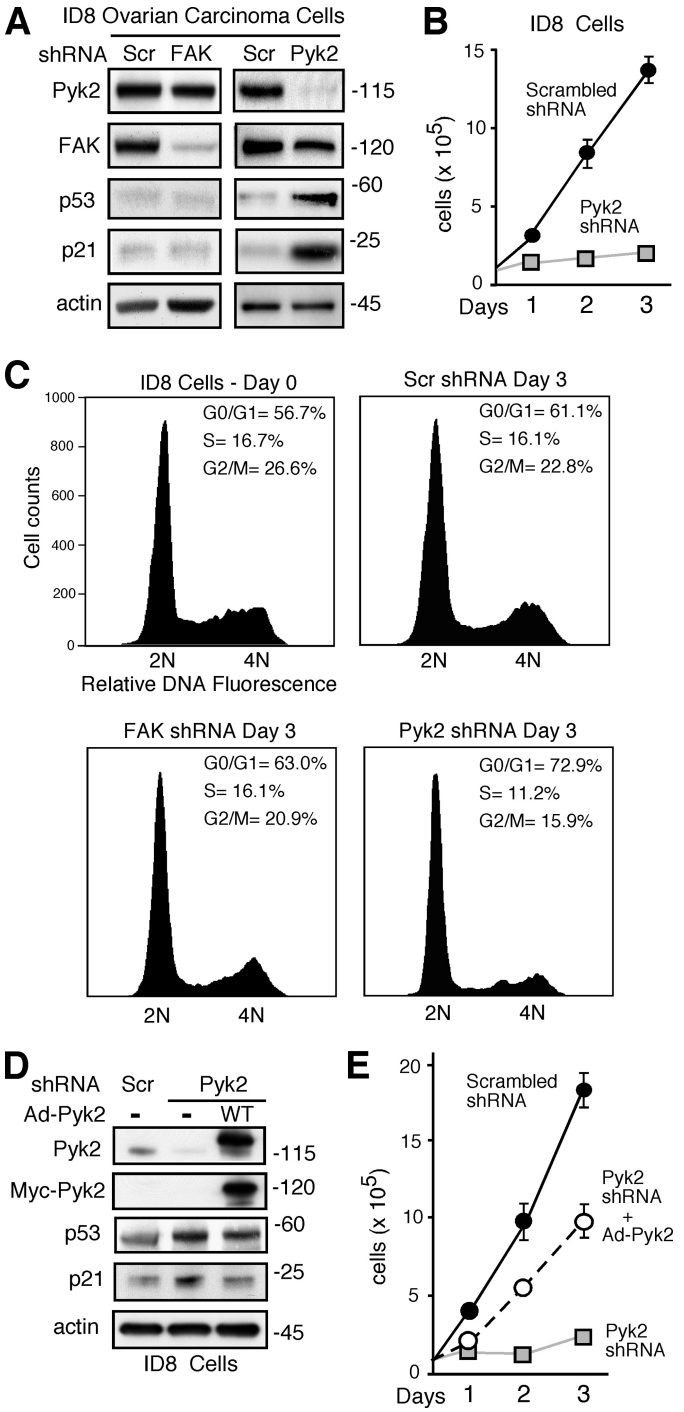

FIGURE 6. **Pyk2 regulation of p53 and ID8 ovarian carcinoma cell growth.** *A*, Pyk2 but not FAK knockdown increases p53 and p21 levels. ID8 cells were transduced with lentiviral Scr, FAK, or Pyk2 shRNA, and after 5 days cell lysates were analyzed by anti-Pyk2, FAK, p53, p21, and actin blotting. *B*, Pyk2 knockdown slows ID8 cell proliferation. ID8 cells were transduced with lentiviral Scr or Pyk2 shRNA and after 48 h analyzed for cell proliferation by cell counting. Results are the mean cell number ± S.D.; $n = 3$ independent experiments. *C*, Pyk2 knockdown triggers G_1 cell cycle arrest. Cell cycle analysis was determined by propidium iodide staining and flow cytometry. Day 0 represents growing cells before lentiviral shRNA expression. Pyk2 but not FAK or Scr shRNA-expressing ID8 cells exhibit G_1 cell cycle arrest after 72 h. *D*, full-length Pyk2 re-expression counteracts ID8 Pyk2 shRNA-associated increases in p53 and p21 levels. ID8 cells were infected with lentiviral-associated Scr or Pyk2 shRNA and after 48 h exposed to either mock or adenoviral Myc-Pyk2. At 96 h, lysates were blotted for Pyk2, p53, p21, Myc, and actin expression. *E*, Ad-Pyk2 full-length WT re-expression in ID8 Pyk2 shRNA cells promotes cell proliferation. After 48 h of Scr and anti-Pyk2 shRNA lentiviral transduction in ID8 cells, cell proliferation was analyzed by counting. Results are the mean values ± S.D., $n = 2$ independent experiments. shRNA-associated, cell cycle analyses, and re-expression experiments were repeated at least two times.

Only Pyk2 FERM-WT promoted enhanced p53 ubiquitination, and this did not occur in $Mdm2^{-/-}$ MEFs. The lack of Pyk2 FERM-TT activity suggests that nuclear localization or p53-Mdm2 binding is required for FERM-enhanced p53 ubiquitination. These results show that Pyk2 FERM promotes p53 turnover through enhanced Mdm2-associated p53 ubiquitination and degradation. These results are also consistent with the hypothesis that Pyk2 FERM serves as nuclear-localized scaffold to promote Mdm2-dependent p53 ubiquitination leading to enhanced p53 proteasomal degradation.

Endogenous Pyk2 Control of ID8 Ovarian Carcinoma Cell Growth—We have shown that after genetic or targeted inhibition of FAK expression, Pyk2 functions to regulate p53 with effects on cell cycle progression. What remains unknown is whether endogenous Pyk2 acts to regulate p53 in cells that express FAK. This question is complicated, as the majority of adherent cell types express high levels of FAK and only low levels of Pyk2. However, Pyk2 expression is elevated in breast (29), prostate (30), and hepatocellular carcinoma tumor progression (31). As such, we screened a variety of tumor cell lines known to express wild-type p53 and found that murine ID8 ovarian carcinoma cells express relatively high levels of both Pyk2 and FAK (Fig. 6*A*).

Surprisingly, FAK shRNA knockdown did not result in detectable changes in ID8 p53 or p21 levels (Fig. 6*A*), nor did it affect ID8 cell growth (data not shown) or cell cycle progression (Fig. 6*C*). In contrast, Pyk2 shRNA knockdown triggered elevated p53 and p21 levels (Fig. 6*A*), inhibited ID8 cell proliferation (Fig. 6*B*), and was associated with an increased percentage of ID8 cells in G_0/G_1 and a decreased percentage in S phase of the cell cycle compared with Scr shRNA controls (Fig. 6*C*). To prove the specificity of the Pyk2 knockdown results, human Myc-tagged Pyk2 was re-expressed in the murine Pyk2 shRNA-expressing ID8 cells. Pyk2 re-expression reversed the rise in p53 and p21 levels (Fig. 6*D*) and also promoted ID8 cell proliferation (Fig. 6*E*) compared with Pyk2 shRNA-expressing ID8 cells. Although it remains unclear why Pyk2 (and not FAK) is connected to p53 regulation in ID8 cells, these results reveal important roles for endogenous Pyk2 in p53 inhibition and the control of cell proliferation in certain cell types.

Pyk2 FERM Inhibition of p53 and p21 with Effects on ID8 BrdUrd Incorporation—To determine whether Pyk2-mediated control of p53 and ID8 cell proliferation is via the Pyk2 FERM domain, re-expression of Pyk2 FERM-WT or Pyk2 FERM-TT were tested for effects on elevated p53 and p21 levels induced by Pyk2 shRNA knockdown (Fig. 7*A*). Importantly, Pyk2 FERM-WT, but not the FERM-TT mutant, reduced p53 levels and blocked p21 expression as an indicator of p53 inhibition. As ID8 Pyk2 shRNA knockdown results in a G_0/G_1 cell cycle block (Fig. 6*C*), FERM domain re-expression was tested for the effects on BrdUrd incorporation as a marker of cell cycle progression (Fig. 7, *B* and *C*). BrdUrd incorporation was significantly reduced in Pyk2 compared with control shRNA ID8 cells (Fig. 7*B*). Pyk2 FERM WT promoted an ~4-fold increase in ID8 Pyk2 shRNA

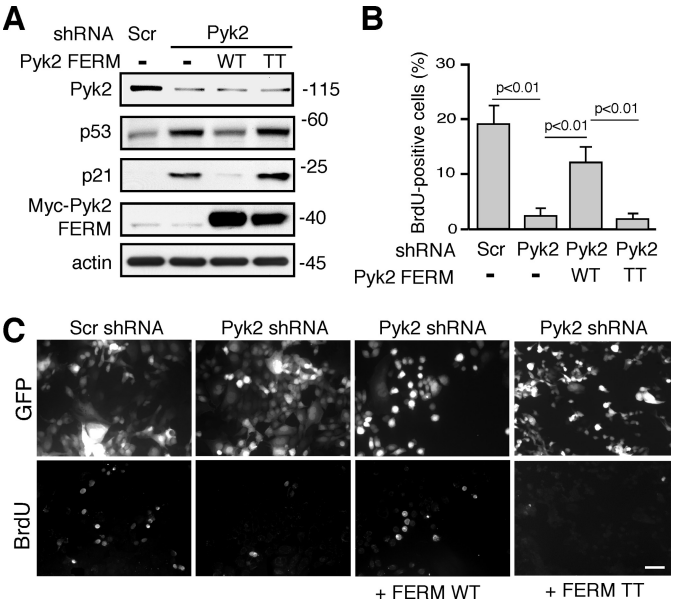

FIGURE 7. **Pyk2 FERM regulation of p53 and ID8 cell growth.** *A*, Ad-Pyk2 FERM expression in ID8 Pyk2 shRNA cells reduces p53 and p21 levels. ID8 cells were transduced with lentiviral Scr or Pyk2 shRNA and after 48 h transduced with adenoviral Myc-Pyk2 FERM WT or Myc-Pyk2 FERM (R184T, R185T, TT). At 96 h cell lysates were blotted for Pyk2, p53, p21, Myc-FERM, and actin levels. *B*, WT Pyk2 FERM rescues ID8 cell proliferation block upon Pyk2 knockdown. ID8 cells were lentiviral- and adenoviral-transduced as in *panel A*, and at 72 h BrdUrd was added for 16 h followed by cell staining with BrdUrd antibody to measure changes in S phase cell cycle progression. Mean values ± S.D.; $n = 3$ independent experiments are the percent of total GFP (from lentiviral shRNA)-positive cells. Significance was determined using analysis of variance and Tukey-Kramer HSD tests. *C*, representative BrdUrd staining images are shown. The *scale bar* is 200 μm. shRNA-associated experiments were repeated at least two times.

cell BrdUrd incorporation, whereas Pyk2 FERM-TT expression had no effect (Fig. 7, *B* and *C*). These results support a conserved role for Pyk2 FERM-mediated regulation of p53 in cell growth control for multiple cell types and independent of cell transformation.

Endogenous Pyk2-p53 Association and Control of ID8 Survival upon Chemical Stress—The protein kinase inhibitor staurosporine promotes rapid FAK nuclear translocation in HUVECs (10). As Pyk2 is important for ID8 cell proliferation, we tested whether Pyk2 regulation of p53 affects ID8 cell survival in the presence of staurosporine (Fig. 8). Whereas Pyk2 is normally perinuclear-distributed, staurosporine (1 μM for 2 h) addition triggered the redistribution of Pyk2 to the nuclear region of cells (Fig. 8*A*). By cell fractionation, staurosporine promoted an ~2.5-fold increase in nuclear Pyk2 accumulation (Fig. 8*B*). Interestingly, p53 levels increased upon staurosporine addition to ID8 cells (Fig. 8*C*), and this was associated with increased Pyk2-p53 association as determined by co-immunoprecipitation analyses (Fig. 8*C*).

We hypothesize that increased Pyk2 nuclear accumulation and association with p53 may be a pro-survival mechanism in response to stress. Accordingly, cells with elevated Pyk2 may delay p53 accumulation and the generation of cell apoptotic signals. To test this hypothesis, Scr and anti-Pyk2 shRNA-expressing ID8 cells were treated with 1 μM staurosporine for the indicated times and then analyzed for annexin V staining as a marker of cell apoptosis (Fig. 8*D*). Under control conditions, Pyk2 shRNA ID8 cells exhibited higher basal levels of annexin V binding (32.2 *versus* 11.7%) compared with Scr control, which is consistent with the slower overall growth rate of Pyk2 shRNA ID8 cells (Fig. 6*B*). After 2.5 h of staurosporine treatment the ratio of Pyk2-Scr shRNA annexin V-positive cells was 40.2 to 13.2%, after 5 h the ratio was 61.3 to 21.9%, and after 12 h the ratio was 75.0 to 30.8% (Fig. 8*D*). These results show that Pyk2 knockdown predisposes ID8 cells to staurosporine-induced apoptosis. Taken together these results support an important and conserved role for nuclear Pyk2 in mediating p53 inhibition associated with enhanced cell growth and survival.

Pyk2 FERM Prevents p53-dependent Apoptosis—Previously, we showed that in human diploid fibroblasts, FAK knockdown combined with cisplatin treatment promotes p53-dependent apoptosis (10). To determine whether Pyk2 FERM can functionally substitute for FAK, human fibroblasts were treated with FAK shRNA, transduced with Ad Myc-Pyk2 FERM WT or Myc-Pyk2 FERM-TT, and treated with cisplatin (Fig. 9). Compared with Scr shRNA-expressing fibroblasts, FAK knockdown results in elevated p53 and p21 expression (Fig. 9*A*) and increased cell death as measured by enumeration of TUNEL stain of GFP-positive lentiviral shRNA-expressing cells (Fig. 9, *B* and *C*). The addition of Pyk2 FERM WT reduced p53 levels, inhibited p21 expression, and blocked cisplatin-stimulated apoptosis (Fig. 9, *A*–*C*). Conversely, Pyk2 FERM-TT overexpression did not alter cisplatin-increased p53 and p21 expression, nor did it significantly prevent cisplatin-induced apoptosis (Fig. 9, *A*–*C*). These results show that Pyk2 FERM F2 lobe function is important in preventing p53-dependent apoptosis.

DISCUSSION

In tissues and cells derived from $FAK^{-/-}$ mice and in fibroblasts from FAK exon 15-deleted mice (32), Pyk2 is expressed, but its role has remained unclear as it does not efficiently promote cell motility as a replacement for FAK. Herein, we show that Pyk2 promotes cell proliferation and survival through FERM domain-mediated nuclear translocation, p53 binding, and enhanced Mdm2-dependent p53 ubiquitination leading to p53 inhibition. Upon genetic FAK inactivation or as a result of FAK knockdown, Pyk2 regulation of p53 acts as a compensatory and/or adaptive cell survival mechanism (Fig. 10). We show that Pyk2 FERM domain expression is sufficient to mediate these effects with Pyk2 FERM F2 lobe integrity and nuclear translocation as important factors. Pyk2 regulation of p53 also promotes cell survival upon cisplatin or staurosporine-induced cell stress. Importantly, we also find that Pyk2 connections to p53 regulation extend to ID8 ovarian carcinoma cells where both Pyk2 and FAK are endogenously expressed. These results reinforce the evolutionary conservation of this unique and important Pyk2-FAK survival pathway not shared by other FERM-containing proteins such as talin. Additionally, this survival pathway is independent of integrin regulation (33), as it requires FERM domain function that through evolution has maintained a high level of conservation (34).

We found that FAK knockdown was associated with a G_1 cell cycle arrest in HUVECs. Within 7 days Pyk2 levels rose under continued FAK knockdown, and this was associated with decreased p53 levels and re-entry of HUVECs into the cell cycle.

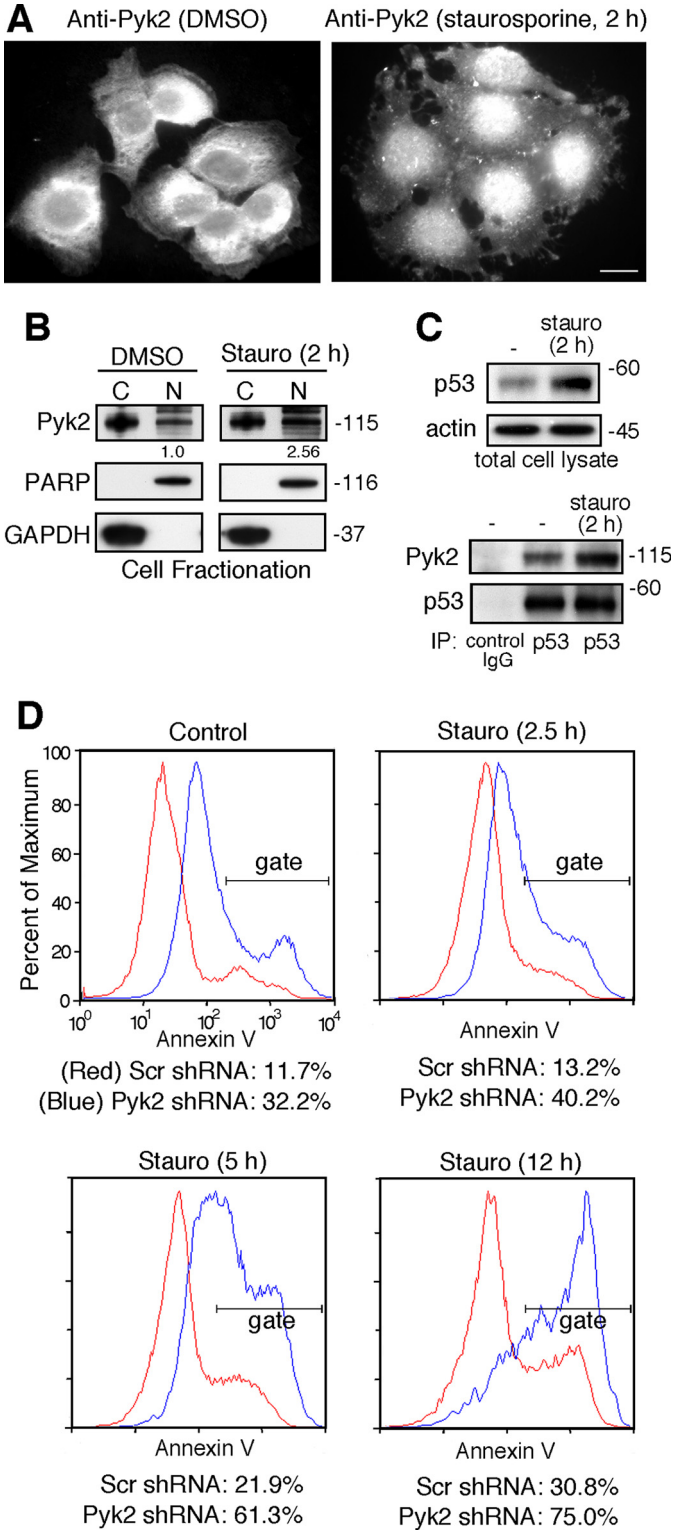

FIGURE 8. **Nuclear-localized Pyk2 associates with p53 and is important for ID8 survival upon staurosporine stress.** *A*, Pyk2 translocates to the nucleus upon staurosporine addition to ID8 cells. Confocal immunofluorescent analysis of endogenous Pyk2 upon DMSO (control) or 1 μM staurosporine addition for 2 h. The *scale bar* is 10 μm. *B*, shown is ID8 cytoplasmic (*C*) and nuclear (*N*) fractionation of Pyk2 distribution upon DMSO or 1 μM staurosporine (*stauro*) addition for 2 h. Antibodies to poly(ADP-ribose) polymerase (*PARP*) and glyceraldehyde-3-phosphate dehydrogenase (*GAPDH*) were used to verify nuclear and cytoplasmic fractionation, respectively. *Numbers below the Pyk2 panels* are densitometric analyses normalized to poly(ADP-ribose) polymerase and DMSO-treated nuclear Pyk2 value was set to 1.0. *C*, increased Pyk2 association with p53 upon ID8 staurosporine stress is shown. Total ID8 cell lysates blotted for p53 and actin levels are shown. *Right*, control mouse IgG or anti-p53 IPs immunoblotted for Pyk2 and p53 before and after staurosporine addition (2 h). *D*, knockdown of Pyk2 increases the rate of ID8 apoptosis after staurosporine (*Stauro*) addition. Scr (*red histogram*) and anti-Pyk2 shRNA (*blue histogram*) expressing ID8 cells were treated with DMSO or 1 μM staurosporine for the indicated times and then analyzed for annexin V binding by flow cytometry. Percent of total annexin V-positive cells within the gated region is indicated. Fractionation, co-IP, and annexin V staining experiments were repeated at least two times.

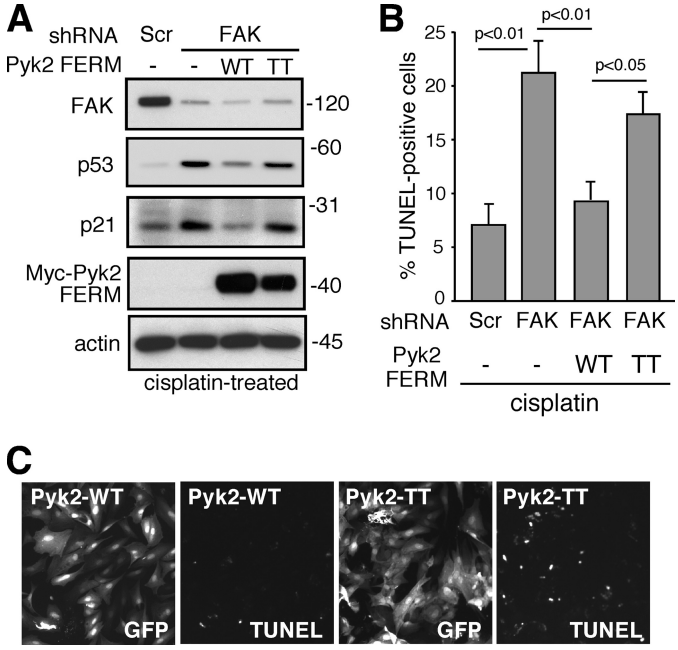

FIGURE 9. **Pyk2 FERM promotes survival after FAK knockdown and cisplatin treatment.** *A*, Pyk2 FERM blocks cisplatin-stimulated increased p53 and p21 levels. Human fibroblasts were transduced with lentiviral Scr or anti-FAK shRNA and after 48 h infected with adenoviral Myc-Pyk2 FERM WT or Myc-Pyk2 FERM (R184T, R185T, TT) (24 h). At 72 h cells were treated with cisplatin (10 μg/ml), and at 96 h, lysates were immunoblotted FAK, p53, p21, Myc tag (Pyk2 FERM), and actin. *B*, human fibroblasts were transduced with the indicated lentiviral shRNA and Ad-Pyk2 FERM as in *A* and treated with cisplatin (20 μg/ml) for an additional 24 h. Cells were analyzed for apoptosis by TUNEL staining. Mean values are the percent of total GFP-positive cells $\pm$ S.D.; $n = 2$ independent experiments. Significance was determined using analysis of variance and Tukey-Kramer HSD tests. *C*, representative images of FAK shRNA-expressing fibroblasts transduced with either Pyk2 FERM WT or Pyk2 FERM TT after cisplatin addition. Shown are GFP (lentiviral shRNA) and TUNEL staining of the same field (10× magnification). shRNA-associated experiments were repeated at least two times.

In both FAK$^{-/-}$p21$^{-/-}$ MEFs and ID8 ovarian carcinoma cells, knockdown of endogenous Pyk2 resulted in elevated p53 levels and cell growth inhibition that was rescued by p53 inactivation or exogenous Pyk2 FERM domain re-expression. Pyk2 FERM associated with p53 and Mdm2 and Pyk2 FERM point mutations (R184T, R185T, TT) decreased these interactions as well as prevented Pyk2 FERM nuclear localization and FERM-enhanced p53 ubquitination. As Pyk2 FERM effects on p53 were blocked by the MG132 proteasome inhibitor, our studies support a role for the Pyk2 FERM domain acting as nuclear scaffold to facilitate p53 degradation.

Importantly, staurosporine-induced cell stress promoted endogenous ID8 Pyk2 nuclear accumulation and Pyk2-p53 interaction. As Pyk2 FERM but not Pyk2 FERM-TT can also rescue cisplatin-triggered and p53-dependent human fibro-

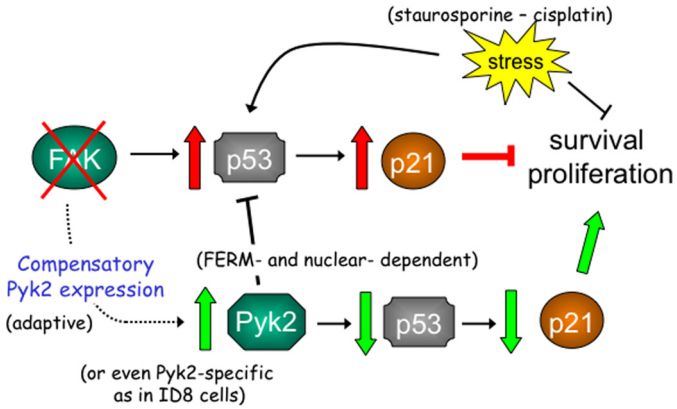

FIGURE 10. **Model of FAK- and/or Pyk2-associated affects on p53 regulating cell proliferation and survival.** Loss of FAK expression leads to elevated p53 levels, p53-mediated activation of targets such as the p21 cyclin-dependent kinase inhibitor, and a block in proliferation detected as a G_0/G_1 cell cycle arrest (*red arrows*). Adaptive or compensatory elevation in Pyk2 levels occur in mice and in cell culture to counteract p53 activation, leading to a reduction in p21 levels and allowing for cell cycle re-initiation as detected by BrdUrd incorporation (*green arrows*). We show that Pyk2 FERM domain expression is sufficient to mediate these effects with Pyk2 FERM F2 lobe integrity and nuclear translocation as important factors. Pyk2 regulation of p53 also promotes cell survival upon cisplatin or staurosporine-induced cell stress. Cells that express high levels of FAK or Pyk2 may be more resistant to apoptotic stimuli by preventing excessive p53 activation.

blast apoptosis, our results support the notion that Pyk2 functions to promote cell survival independently of FAK.

Our results also add a new level of complexity to the interpretation of FAK knock-out mice phenotypes. For instance, inactivation of FAK in ECs during development has yielded lethal phenotypes with growth defects in culture potentially due to p53 activation (9, 35), whereas conditional inactivation of FAK in adult mouse ECs yields no distinct phenotype in part as a result of up-regulated Pyk2 expression (17). Similarly, conditional FAK knock-out in skin has yielded keratinocytes that show high levels of apoptosis in cell culture (36, 37), whereas another group has successfully established $FAK^{-/-}$ keratinocytes in culture by growing on feeder cells (38). Notably, feeder-initiated $FAK^{-/-}$ keratinocytes express Pyk2, and these cells exhibit elevated levels of Rho GTPase activity compared with normal keratinocytes. This phenotype is very similar to that of $FAK^{-/-}p53^{-/-}$ MEFs where Pyk2 kinase-dependent signaling promotes elevated expression of the guanine nucleotide exchange factor, p190RhoGEF (18).

Another question raised by our studies is whether there may be biologically relevant roles for the generation of N-terminal fragments of Pyk2 or FAK. Interestingly, alternative FAK transcripts (containing exon 18a) with a premature stop codon have been detected in human brain corresponding to a putative FAK protein encompassing the FAK FERM domain (34). However, cellular and environmental context may dictate whether FAK or Pyk2 FERM domains function in a positive or negative fashion. This is due to the fact that FAK FERM overexpression can inhibit FAK tyrosine phosphorylation in trans (39) and block FAK signaling, promoting cytokine gene expression (40). Expression of the Pyk2 FERM domain can similarly function to inhibit Pyk2 phosphorylation as well as reduce glioma tumor progression (41, 42). Exogenous Pyk2 FERM also inhibits Pyk2 kinase activity in cardiomyocytes, leading to the inhibition of phenylephrine-induced atrial natriuretic factor secretion (43). Interestingly, FAK negatively regulates atrial natriuretic factor secretion in cardiomyocytes, suggesting that Pyk2 and FAK can make distinct signaling connections when co-expressed in cells.

This separation of function for Pyk2-FAK is consistent with our findings in ID8 carcinoma cells where Pyk2 and FAK are equally expressed, but only Pyk2 was selectively was connected to p53 regulation. Because ~50% of ovarian cancers contain wild-type p53 (44), elevated FAK levels and tyrosine phosphorylation are associated with invasive ovarian cancer (45), and Pyk2 signaling has been connected to increased ovarian carcinoma telomerase activity (46), future studies will be aimed at elucidating both the conserved and differential signaling roles of FAK and Pyk2 in ovarian cancer tumor progression.

Acknowledgments—We thank Erik Goka and Sara Weis for lung lysates from WT and inducible EC-specific FAK knock-out mice and Dusko Ilic for $FAK^{-/-}p21^{-/-}$ MEFs and for critical review. $Mdm2^{-/-}p53^{-/-}$ MEFs were provided by Stephen Jones (University of Massachusetts Medical School) through the generosity of Ze'ev Ronai (Burnham Institute). We appreciate administrative assistance from Susie Morris, and we thank Alok Tomar and Christine Lawson for helpful comments.

REFERENCES

1. Parsons, J. T. (2003) *J. Cell Sci.* **116,** 1409–1416
2. Avraham, H., Park, S. Y., Schinkmann, K., and Avraham, S. (2000) *Cell. Signal.* **12,** 123–133
3. Mitra, S. K., Hanson, D. A., and Schlaepfer, D. D. (2005) *Nat. Rev. Mol. Cell Biol.* **6,** 56–68
4. Sieg, D. J., Ilić, D., Jones, K. C., Damsky, C. H., Hunter, T., and Schlaepfer, D. D. (1998) *EMBO J.* **17,** 5933–5947
5. Klingbeil, C. K., Hauck, C. R., Hsia, D. A., Jones, K. C., Reider, S. R., and Schlaepfer, D. D. (2001) *J. Cell Biol.* **152,** 97–110
6. Ostergaard, H. L., and Lysechko, T. L. (2005) *Immunol. Res.* **31,** 267–282
7. Kohno, T., Matsuda, E., Sasaki, H., and Sasaki, T. (2008) *Biochem. J.* **410,** 513–523
8. Ilić, D., Furuta, Y., Kanazawa, S., Takeda, N., Sobue, K., Nakatsuji, N., Nomura, S., Fujimoto, J., Okada, M., Yamamoto, T., and Aizawa, S. (1995) *Nature* **377,** 539–544
9. Ilic, D., Kovacic, B., McDonagh, S., Jin, F., Baumbusch, C., Gardner, D. G., and Damsky, C. H. (2003) *Circ. Res.* **92,** 300–307
10. Lim, S. T., Chen, X. L., Lim, Y., Hanson, D. A., Vo, T. T., Howerton, K., Larocque, N., Fisher, S. J., Schlaepfer, D. D., and Ilic, D. (2008) *Mol. Cell* **29,** 9–22
11. Vousden, K. H. (2002) *Biochim. Biophys. Acta* **1602,** 47–59
12. Iwakuma, T., and Lozano, G. (2003) *Mol. Cancer Res.* **1,** 993–1000
13. Lim, S. T., Mikolon, D., Stupack, D. G., and Schlaepfer, D. D. (2008) *Cell Cycle* **7,** 2306–2314
14. Golubovskaya, V. M., Finch, R., and Cance, W. G. (2005) *J. Biol. Chem.* **280,** 25008–25021
15. Oren, M. (2003) *Cell Death Differ.* **10,** 431–442
16. Vogelstein, B., Lane, D., and Levine, A. J. (2000) *Nature* **408,** 307–310
17. Weis, S. M., Lim, S. T., Lutu-Fuga, K. M., Barnes, L. A., Chen, X. L., Göthert, J. R., Shen, T. L., Guan, J. L., Schlaepfer, D. D., and Cheresh, D. A. (2008) *J. Cell Biol.* **181,** 43–50
18. Lim, Y., Lim, S. T., Tomar, A., Gardel, M., Bernard-Trifilo, J. A., Chen, X. L., Uryu, S. A., Canete-Soler, R., Zhai, J., Lin, H., Schlaepfer, W. W., Nalbant, P., Bokoch, G., Ilic, D., Waterman-Storer, C., and Schlaepfer, D. D. (2008) *J. Cell Biol.* **180,** 187–203
19. Roby, K. F., Taylor, C. C., Sweetwood, J. P., Cheng, Y., Pace, J. L., Tawfik, O., Persons, D. L., Smith, P. G., and Terranova, P. F. (2000) *Carcinogenesis* **21,** 585–591

20. Mitra, S. K., Lim, S. T., Chi, A., and Schlaepfer, D. D. (2006) *Oncogene* **25,** 4429–4440
21. Oktay, M., Wary, K. K., Dans, M., Birge, R. B., and Giancotti, F. G. (1999) *J. Cell Biol.* **145,** 1461–1469
22. Mettouchi, A., Klein, S., Guo, W., Lopez-Lago, M., Lemichez, E., Westwick, J. K., and Giancotti, F. G. (2001) *Mol. Cell* **8,** 115–127
23. Zhao, J., Pestell, R., and Guan, J. L. (2001) *Mol. Biol. Cell* **12,** 4066–4077
24. Lietha, D., Cai, X., Ceccarelli, D. F., Li, Y., Schaller, M. D., and Eck, M. J. (2007) *Cell* **129,** 1177–1187
25. Lipinski, C. A., Tran, N. L., Dooley, A., Pang, Y. P., Rohl, C., Kloss, J., Yang, Z., McDonough, W., Craig, D., Berens, M. E., and Loftus, J. C. (2006) *Biochem. Biophys. Res. Commun.* **349,** 939–947
26. Aoto, H., Sasaki, H., Ishino, M., and Sasaki, T. (2002) *Cell Struct. Funct.* **27,** 47–61
27. Faure, C., Corvol, J. C., Toutant, M., Valjent, E., Hvalby, O., Jensen, V., El Messari, S., Corsi, J. M., Kadaré, G., and Girault, J. A. (2007) *J. Cell Sci.* **120,** 3034–3044
28. Ossovskaya, V., Lim, S. T., Ota, N., Schlaepfer, D. D., and Ilic, D. (2008) *FEBS Lett.* **582,** 2402–2406
29. Behmoaram, E., Bijian, K., Jie, S., Xu, Y., Darnel, A., Bismar, T. A., and Alaoui-Jamali, M. A. (2008) *Am. J. Pathol.* **173,** 1540–1550
30. Iiizumi, M., Bandyopadhyay, S., Pai, S. K., Watabe, M., Hirota, S., Hosobe, S., Tsukada, T., Miura, K., Saito, K., Furuta, E., Liu, W., Xing, F., Okuda, H., Kobayashi, A., and Watabe, K. (2008) *Cancer Res.* **68,** 7613–7620
31. Sun, C. K., Man, K., Ng, K. T., Ho, J. W., Lim, Z. X., Cheng, Q., Lo, C. M., Poon, R. T., and Fan, S. T. (2008) *Carcinogenesis* **29,** 2096–2105
32. Corsi, J. M., Houbron, C., Billuart, P., Brunet, I., Bouvree, K., Eichmann, A., Girault, J. A., and Enslen, H. (2009) *J. Biol. Chem.* **284,** 34769–34776
33. Gilmore, A. P., Owens, T. W., Foster, F. M., and Lindsay, J. (2009) *Curr. Opin. Cell Biol.* **21,** 654–661
34. Corsi, J. M., Rouer, E., Girault, J. A., and Enslen, H. (2006) *BMC Genomics* **7,** 198
35. Shen, T. L., Park, A. Y., Alcaraz, A., Peng, X., Jang, I., Koni, P., Flavell, R. A., Gu, H., and Guan, J. L. (2005) *J. Cell Biol.* **169,** 941–952
36. McLean, G. W., Komiyama, N. H., Serrels, B., Asano, H., Reynolds, L., Conti, F., Hodivala-Dilke, K., Metzger, D., Chambon, P., Grant, S. G., and Frame, M. C. (2004) *Genes Dev.* **18,** 2998–3003
37. Essayem, S., Kovacic-Milivojevic, B., Baumbusch, C., McDonagh, S., Dolganov, G., Howerton, K., Larocque, N., Mauro, T., Ramirez, A., Ramos, D. M., Fisher, S. J., Jorcano, J. L., Beggs, H. E., Reichardt, L. F., and Ilic, D. (2006) *Oncogene* **25,** 1081–1089
38. Schober, M., Raghavan, S., Nikolova, M., Polak, L., Pasolli, H. A., Beggs, H. E., Reichardt, L. F., and Fuchs, E. (2007) *J. Cell Biol.* **176,** 667–680
39. Cohen, L. A., and Guan, J. L. (2005) *J. Biol. Chem.* **280,** 8197–8207
40. Schlaepfer, D. D., Hou, S., Lim, S. T., Tomar, A., Yu, H., Lim, Y., Hanson, D. A., Uryu, S. A., Molina, J., and Mitra, S. K. (2007) *J. Biol. Chem.* **282,** 17450–17459
41. Lipinski, C. A., Tran, N. L., Viso, C., Kloss, J., Yang, Z., Berens, M. E., and Loftus, J. C. (2008) *J. Neurooncol.* **90,** 181–189
42. Loftus, J. C., Yang, Z., Tran, N. L., Kloss, J., Viso, C., Berens, M. E., and Lipinski, C. A. (2009) *Mol. Cancer Ther.* **8,** 1505–1514
43. Menashi, E. B., and Loftus, J. C. (2009) *Cell Tissue Res.* **337,** 243–255
44. Landen, C. N., Jr., Birrer, M. J., and Sood, A. K. (2008) *J. Clin. Oncol.* **26,** 995–1005
45. Sood, A. K., Coffin, J. E., Schneider, G. B., Fletcher, M. S., DeYoung, B. R., Gruman, L. M., Gershenson, D. M., Schaller, M. D., and Hendrix, M. J. (2004) *Am. J. Pathol.* **165,** 1087–1095
46. Alfonso-De Matte, M. Y., and Kruk, P. A. (2004) *Cancer Res.* **64,** 23–26

PYK2 INHIBITION OF P53 AS AN ADAPTIVE AND INTRINSIC MECHANISM FACILITATING CELL PROLIFERATION AND SURVIVAL

Ssang-Taek Lim[1#], Nichol L. G. Miller[1#], Ju-Ock Nam[1#], Xiao Lei Chen[1], Yangmi Lim[2], and David D. Schlaepfer[1,3]

[1]University of California San Diego, Moores Cancer Center, Department of Reproductive Medicine

[2]Current Address: Mogam Research Institute, 341 Bojeong-dong, Giheung-gu, Yongin, 446-799, Korea

[#]These authors contributed equally to this study. Running head: Pyk2 FERM regulation of p53

[3]Address correspondence to: David D. Schlaepfer, Ph.D., University of California San Diego, Moores Cancer Center, Department of Reproductive Medicine, 0803, 3855 Health Sciences Dr., La Jolla, CA 92093. Fax: (858) 822-7519, E-mail: dschlaepfer@ucsd.edu

Legends to Supplemental Figures

Table I. Primers used for PCR cloning, PCR mutagenesis and lentiviral shRNA knockdown.

Supplemental Figure. 1. **FAK knockdown in HUVECs.** (A) Loss of FAK does not trigger apoptosis. Allophycocyanin-conjugated annexin V staining of growing (Day 0, filled) or staurosporine-treated (1 μM, 12 h) HUVECs shown as negative and positive controls, respectively. Lentiviral-mediated expression of FAK and Scr shRNA were evaluated for effects on cell apoptosis after 4 and 7 days. Knockdown of FAK (red line) did not increase annexin V staining compared to Scr control (blue line), annexin positive population was gated. The gated region was constant and was set using staurosporine treatment of HUVECs. (B) FAK, Pyk2, p53 levels after lentiviral-mediated anti-FAK or control scrambled (Scr) shRNA expression in HUVECs as determined. Actin was used as a loading control. Days 4 or 7 are time after initial infection.

Supplemental Figure 2. **Pyk2 knockdown does not increase FAK-/-p21-/- MEF apoptosis.** APC-annexin V staining of growing (Day 0, filled) or staurosporine-stressed (1 μM, 12 h) FAK-/-p21-/- fibroblasts shown as negative and positive controls, respectively. Lentiviral-mediated expression of Scr or Pyk2 shRNA were evaluated for effects on cell apoptosis after 3 days. Pyk2 knockdown did not increase annexin V staining compared to Scr control. The gated region was constant and was set using staurosporine treatment. (B) Pyk2 shRNA-expressing FAK-/-p21-/- MEFs grow slower than scrambled shRNA control. Passage 10 FAK-/-p21-/- MEFs were transduced with different anti-mouse lentiviral Pyk2 shRNA constructs and cell growth over 4 days was compared to scrambled (Scr) control shRNA. Resulting cell counts from 3 dishes at each experimental day are mean cell number ± SD.

Supplemental Table 1. Primers used for PCR cloning, PCR mutagenesis and shRNA.

Primer	Sequence	Note
Pyk2_BglI-5'	5'-gcaggagatctcgtatcctcaaggtctgcttc-3'	Pyk2 39-367 cloning BglI underlined
Pyk2_XbaI-3'	5'-gctcgtctagacctaggatggatgatgagaga-3	Pyk2 39-367 cloning XbaI underlined
Pyk2 FERM R184T/R185T-5'	5'-cagctgggctgcctggagttaacgacgttcttcaaggatat-3'	R184T/R185Tmutagenesis Mutated sequences underlined
Pyk2 FERM R184T/R185T-3'	5'-tttaagctttacctaggatggatgatgagagagccttg-3'	R184T/R185Tmutagenesis Mutated sequences underlined
Pyk2_FERM_HindIII-5'	5'-tttaagcttcgtatcctcaaggtctgcttctatagc-3'	Ad-Myc-Pyk2 FERM subcloning HindIII underlined
Pyk2_FERM_HindIII-3'	5'-tttaagctttacctaggatggatgatgagagagccttg-3'	Ad-Myc-Pyk2 FERM subcloning HindIII underlined
Mouse Pyk2 shRNA-5' #1	5'-*t*GAAGTAGTTCTTAACCGCA*ttcaagaga*TGCGGTTAAGAACTA CTTC*tttttt*c-3'	shRNA cloning
Mouse Pyk2 shRNA-3' #1	5'-TCGA*gaaaaaa*GAAGTAGTTCTTAACCGCATC*tctcttgaa*TGCGG TTAAGAACTACTTC*a*-3'	5'TCGA is XhoI overhang
Mouse Pyk2 shRNA-5' #2	5'-*t*AGCCTCTGTGACACGTCTA*ttcaagaga*TAGACGTGTCACAGA GGCT*tttttt*c-3'	shRNA cloning
Mouse Pyk2 shRNA-3' #2	5'-TCGA*gaaaaaa*GAAGTAGTTCTTAACCGCATC*tctcttgaa*GTGCG GTTAAGAAGAACTA*a*-3'	5'TCGA is XhoI overhang
Mouse FAK shRNA-5' #1	5'-*t*GAATGGCAGCTGCTTATCTT*tcaagag*AAGATAAGCAGCTGCC ATTC*tttttt* c-3	shRNA cloning
Mouse FAK shRNA-3' #1	5'-TCGA*gaaaaaa*GAATGGCAGCTGCTTATCTT*ctcttga*AAGATAAG CAGCTGCCATTCa-3'	5'TCGA is XhoI overhang
Mouse FAK shRNA-5' #2	5'-*t*GAAGGGATCAGTTACCTGA*ttcaagaga*TCAGGTAACTGATCCC TTCTT*tttt*c-3'	shRNA cloning
Mouse FAK shRNA-3' #2	5'-TCGAgaaaaaaGAAGGGATCAGTTACCTGATCttgaaTCAGGTAA CTGATCCCTTCa-3'	5'TCGA is XhoI overhang
Human FAK shRNA-5' #1	5'-tGAACCTCGCAGTCATTTATTtcaagagAATAAATGACTGCGA GGTTCttttttc-3'	shRNA cloning
Human FAK shRNA-3' #1	5'-TCGAgaaaaaaGAACCTCGCAGTCATTTATTctcttgaAATAAATGAC TGCGAGGTTCa-3'	5'TCGA is XhoI overhang
Human FAK shRNA-5' #2	5'-tGGCATTTATATGAGTCCAGTtcaagagACTGGACTCATATAAA TGCCTttttc-3'	shRNA cloning
Human FAK shRNA-5' #2	5'-TCGAgaaaaaaGAACCTCGCAGTCATTTATTCAGTCtcttgaaCTGG ACTCATATAAATGCCa3'	5'TCGA is XhoI overhang

5' primer represents forward and 3' for reverse primers. Italicized characters are accessory components of shRNA.

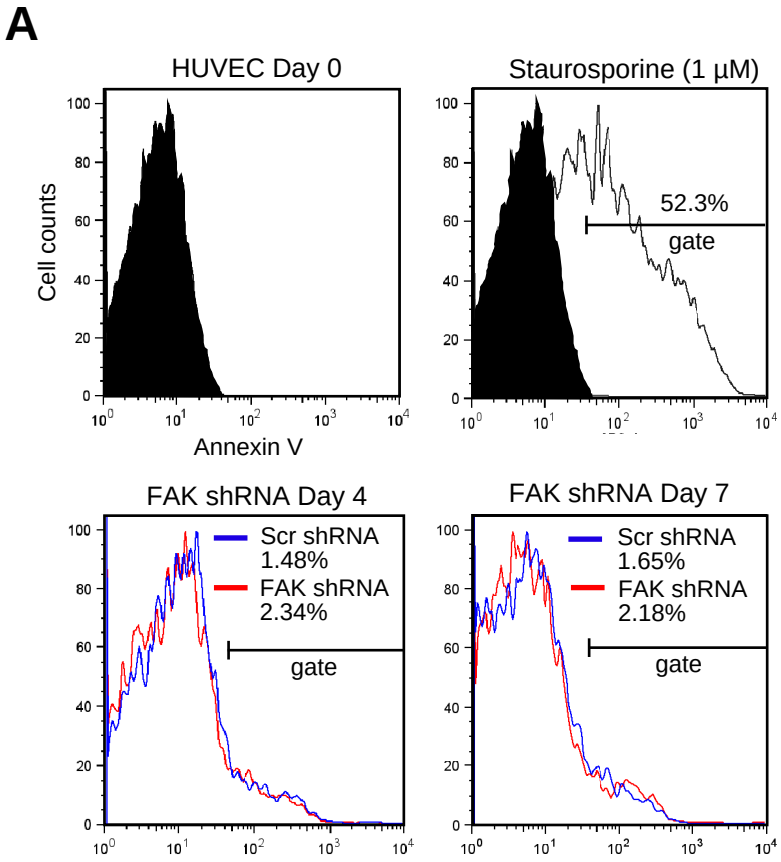

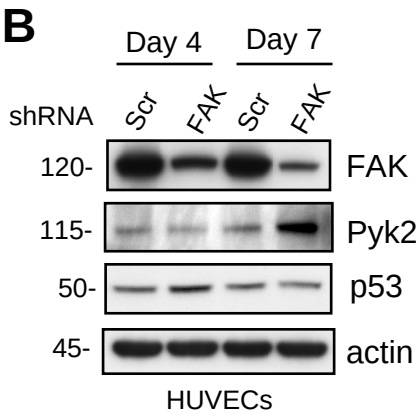

Supplemental Figure 1

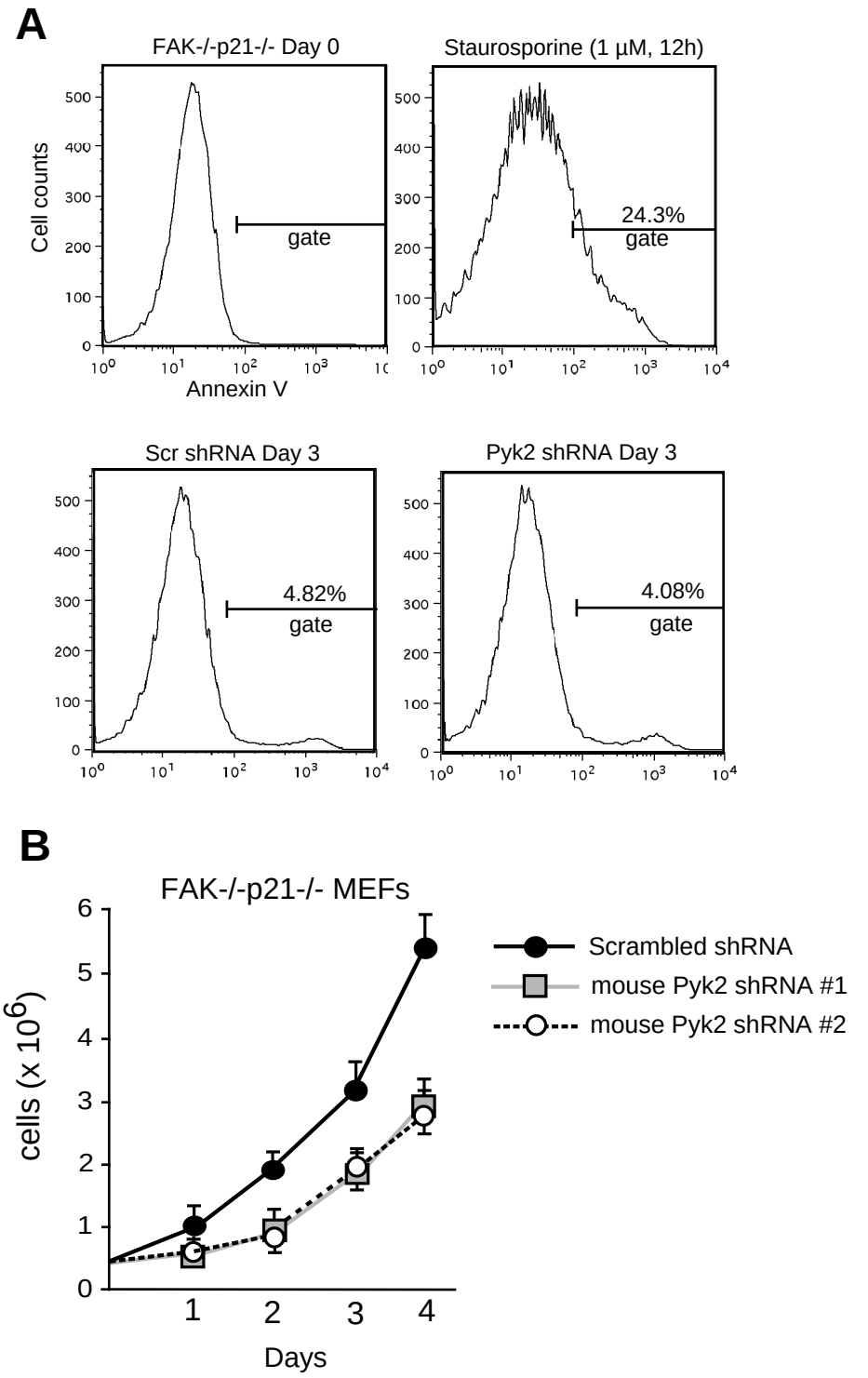

Supplemental Figure 2